INDIAN JOURNAL OF SCIENCE AND TECHNOLOGY

RESEARCH ARTICLE

Rate Equations Model to Simulate the Dual Generation of Nd^{+3}: YAG Passive Q-Switched Laser Pulses

Sara Abdulhussain[1], Abdul-Kareem Mahdi Salih[2]*

1 Bio medical Department, College of Engineering- University of Thi-Qar, Thi-Qar, Iraq
2 Physics Department, College of Science - University of Thi-Qar, Thi-Qar, Iraq

OPEN ACCESS

Received: 02-08-2023
Accepted: 04-09-2023
Published: 27-10-2023

Citation: Abdulhussain S, Salih AKM (2023) Rate Equations Model to Simulate the Dual Generation of Nd^{+3}: YAG Passive Q-Switched Laser Pulses. Indian Journal of Science and Technology 16(40): 3462-3470. https://doi.org/10.17485/IJST/v16i40.1748

* **Corresponding author**.

abdulkareem@sciutq.edu.iq

Funding: None

Competing Interests: None

Published By Indian Society for Education and Environment (iSee)

ISSN
Print: 0974-6846
Electronic: 0974-5645

Abstract

Objective: Rate equations model has been formulated to simulate the simultaneous generation of two passive Q-switching pulses using one active medium. It is possible to separate them and employ each pulse in practical applications. **Methods:** The model was solved numerically by used Rung–kutta–Fahelberg method. This model was tested in the study of the effect of saturable absorber $(Cr^{+4} : YAG)$ ions concentration on the duration, energy, and power of the dual pulses which are generation by passive Q-switching of $Nd^{+3} : YAG$. **Finding**: The results of the numerical solution showed that the temporal behavior of photons density of passive Q-switching pulses and the population inversion density of active medium is good agreement with studies which dealt the theory of passive Q-switching, which enhances reliability using this model. **Novelty**: The mathematical model included six rate equations instead of three or four rate equations. It is based to simulate the ${}^4F_{3/2}$, ${}^4I_{11/2}$, ${}^4I_{9/2}$ spectrum lines as a 4-level and 3-level energy schemes of $Nd^{+3} : YAG$ active medium to get two passive Q-switching laser pulses at the same time (instantaneously) instead of one pulse. Can be separated into two pulses to employ each of them in applications.
Keywords: Laser; Passive Q-Switching; Solid state lasers; Nd^{+3}

1 Introduction

Passive Q-switching (PQS) lasers technique exhibits many advantages, such as simple structure, small size, low coast, improved durability and reliability, and does not require complex extra-cavity modulation devices. It produces short pulses and high peak powers[1,2] that have made it widely applied. The applications of this technique are: high-precision processing, laser medical treatment, space detection, radar, and laser communication[3–5]. Materials commonly used for PQS are organic dyes, doped crystals, and semiconductors[4–6]. The Neodymium (ND^{+3}) additive to another host for using active medium laser is the one of commonly used type of the solid state laser[5–7]. ND^{+3} ions doped fiber (AM) used as active medium in this study. The main laser transition in ND^{+3} ions occurs between the upper spectrum line ${}^4F_{3/2}$ manifold to spectrum line ${}^4I_{11/2}$ manifold referred as R_2 at 1064 nm, this transition represents four

level scheme. While the laser transition which occurs between the upper stark level of the $^4F_{3/2}$ manifold to stark level within the $^4I_{9,2}$ manifold referred as R_1 at 946 *nm*, this transition represents three level scheme Nd^{+3} ions are excited from the ground state to the pump band, then followed by a rapid relaxation via multi phonon emission through non-radioactive processes to the upper metastable laser level $^4F_{3/2}$ manifold. The $^4F_{3/2}$ level is split into two stark levels R_1 and R_2, and hence their population exist in a Boltzmann distribution. Lasing takes place from $^4F_{3/2}$ to $^4I_{11/2}$ or $^4I_{9/2}$ spectrum lines as a four and quise-three levels schemes respectively. However, there population is replenished by thermal transition until both levels are depleted[7,8], resulting in the emission of photons, has 1064 *nm* and 964 *nm* wavelength as shown in Figure 1. PQS technique using saturable absorber (SA) is one of the techniques that can be utilized in obtaining high power pulses, Cr^{+4} : *YAG* has wide absorption band, it is an excellent SA material for passive Q-switching in the wavelength range 800 *nm* to 1200 *nm*.[8] The SA of Cr^{+4} : *YAG* was used in this study, is a typical 4-level system as shown in Figure 2[7,9]. The transition from the ground E_1 to E_3 and E_2 to E_4 dependent on the absorption cross sections of E_1 and E_2 levels $(\sigma_{sg}, \sigma_{se})$ respectively. The lifetime of the levels E_3 and E_4 are assumed to be short compared with lifetime of E_2 level (τ_{se}). These three parameters σ_{sg}, σ_{se} and τ_{se} can well describe the dynamics of the SA[7].

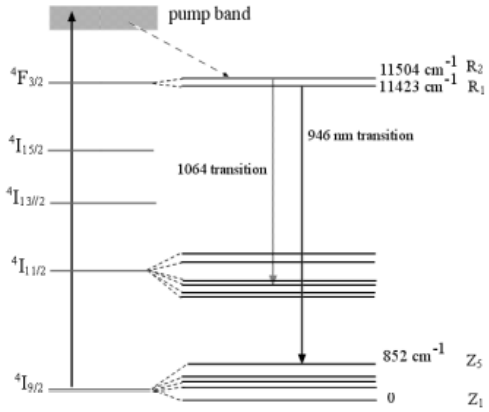

Fig 1. Energy level schemes of ND^{+3} showing Both the 1064 nm and the 946 nm line[8]

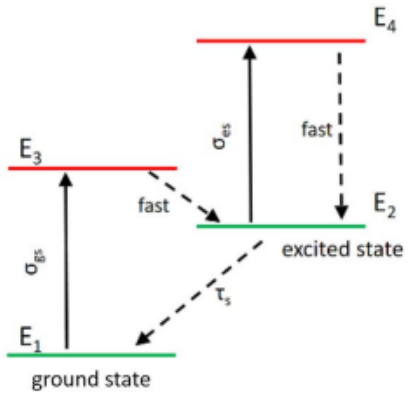

Fig 2. Energy-levels scheme of Cr^{+4}:YAG as a saturable absorber[7,9]

2 Methodology

The mathematical rate equations model of PQS has been presented in this study included six rate equations. The novelty represents the development of rate equations models consisting of three equations as the reference [10–12], or four equations as the reference [13,14]. The model based to simulate the ${}^4F_{3/2}$, ${}^4I_{11/2}$, ${}^4I_{9/2}$ spectrum lines as a 4-level energy schemes (the transition from spectrum line ${}^4F_{3/2}$ to spectrum line ${}^4I_{11/2}$) and 3-level energy schemes (the transition from spectrum line ${}^4F_{3/2}$ to spectrum line ${}^4I_{9/2}$) of $Nd^{+3}:YAG$ active medium to get two passive Q-switching laser pulses instantaneously instead of one pulse as in previous mathematical models. The model was tested by using it in numerical simulation of a laser system consist of $Nd^{+3}:YAG$ used as AM and $Cr^{+4}:YAG$ as a SA. The temporal behavior of each photons density of passive Q-switching pulse and population inversion density of AM ions resulting from the simulation showed good agreement with studies which dealt the theory of passive Q-switching [15–17]. This benchmark enhances reliability using the model.

3 Theory

The presented rate equations model as the following:

$$\frac{d\varphi_1}{dt} = \varphi_1 \left(K_{am1}N_{g1} - K_{sg1}n_{sg} - K_{se1}n_{se} - \gamma_{c1}\right] \tag{1}$$

$$\frac{d\varphi_2}{dt} = \varphi_2 \left(K_{am2}N_{g2} - K_{sg2}n_{sg} - K_{se2}n_{se} - \gamma_{c2}\right] \tag{2}$$

$$\frac{dN_{g1}}{dt} = R_p - \gamma_{p1}K_{am1}N_{g1}\varphi_1 + N_{g1}/\tau_g \tag{3}$$

$$\frac{dN_{g2}}{dt} = R_p - \gamma_{p2}K_{am2}N_{g2}\varphi_2 + N_{g2}/\tau_g \tag{4}$$

$$\frac{dn_{sg}}{dt} = -K_{sg1}n_{sg}\varphi_1 - K_{sg2}n_{sg}\varphi_2 + n_{se}/\tau_g \tag{5}$$

$$\frac{dn_{se}}{dt} = K_{sg1}n_{sg}\varphi_1 + K_{sg2}n_{sg}\varphi_2 - n_{se}/\tau_g \tag{6}$$

where φ_1, φ_2 is the photons density $\left(cm^{-3}\right)$ of PQS pulses which are generated from λ_1, λ_2 laser respectively (φ_1 belong to 4 -level scheme, while φ_2 belong to 3-level scheme). N_{g_1} is the population inversion density (PID) of ions $\left(cm^{-3}\right)$ between ${}^4F_{3/2}$ and ${}^4F_{11/2}$ spectrum lines. N_{g2} is the PID of ions between ${}^4F_{3/2}$ and ${}^4F_{9/2}$ spectrum lines. $K_{ami(i=1,2)} = \frac{2\sigma_{ai}l_{am}}{\tau_r}$ is the coupling coefficient between the φ_1, φ_2 photons and the ions of excited level of $AM\left({}^4F_{3/2}\right)$. σ_{ai} is the emission cross sections $\left(cm^2\right)$ of AM at 4-energy level, 3- energy level schemes, l_{am} is the length of AM. $\tau_r = \frac{2l_c}{c}$ is the round trip transit time, l_c is the cavity optical length. c is the speed of light in vacuum. $K_{sgj(j=1,2)} = \frac{2\sigma_{sgj}l_s}{\tau_r}$ is the coupling coefficient between φ_i photons and the ground state ions of SA respectively. $K_{sej(j=1,2)} = \frac{2\sigma_{sej}l_s}{\tau_r}$ is the coupling coefficient between φ_i and the excited state ions of SA respectively. $\sigma_{sg(j=1,2)}$ is the absorption cross sections $\left(cm^2\right)$of ground state of SA, $\sigma_{sej(j=1,2)}$ is the absorption cross sections $\left(cm^2\right)$ of excited state of SA, l_s is the length of SA. $\gamma_{cj(j=1,2)} = \left(ln\frac{1}{R_j} + L_j\right)$ is the cavity decay rate represents the sum of losses in φ_j because of the reflectivity (R_j), absorption and scattering mechanisms in cavity (L_j). $\gamma_{pj(j=1,2)}$ is the reduction population factor equals 1,2 for four and three energy levels schemes of AM system respectively n_{sg}, n_{se} the ions population (No. of ions density) of the ground and excited levels of SA respectively. τ_g the fluorescence lifetime of the upper laser level $\left({}^4F_{3/2}\right)$, τ_{se} the lifetime of the SA. R_P is the pumping rate. The build-up time of PQS laser pulses in generally very short compared the τ_g and R_P [13], then it is possible to neglect the terms of pumping rate and spontaneous decay of the upper laser level (term land term

3 in Equations (3) and (4)) during pulse generation, so τ_{se} is very long compared the build-up time of PQS laser pulses [1], then it is possible to neglect the third terms of Equations (5) and (6).

The initial population inversion density (IPID) between the spectral lines $^4F_{3/2}$ and $^4F_{11/2}(N_{g01})$, $^4F_{3/2}$ and $^4F_{9/2}(N_{g02})$ can be estimated at initial time by boundary conditions, $n_{sg} \approx n_o$ or $n_{se} \approx 0$, where $(n_i = n_{sg} + n_{se})$ is the total ions of SA. $\frac{d\varphi_i}{dt} \approx 0$ in Equations (1) and (2) because of φ_j is very low in value, then the IPID values N_{g01}, N_{g02} for laser medium can be predicted from Equations (1) and (2) respectively, as the following:

$$N_{g0j(j=1,2)} = \frac{K_{sgj} n_i + \gamma_{c1}}{K_{amj}} \tag{7}$$

Threshold population inversion (TPID) for the four and three levels schemes N_{th1}, N_{th2}, respectively can be estimated at time of maximum photons density (when the number of photons inside the optical laser cavity reaches to peak of pulse) by Equations (1) and (2). At TPID the most of SA ions population in the excited state (n_{se}), can be regards $n_{se} \approx n_i$ ($n_{sg} \approx 0$); then can be considering $\frac{d\varphi_j}{dt} \approx 0$, to get:

$$N_{thj(j=1,2)} = \frac{K_{sei} n_i + \gamma_{cj}}{K_{amj}} \tag{8}$$

The pulse energy can be estimated by the expression.

$$E_j = \frac{(N_{goj} - N_{gfj})}{\gamma_j} \frac{(N_{goj} - N_{gfj})\, hvj}{N_{oj}} \tag{9}$$

Where N_{gf} is the final population inversion density (FIPD) it is get from computations. The pulse power can be estimated by the equation:

$$P_j \approx -\frac{hv_j \gamma_{cj}}{\gamma_j} \left[N_{thj} - N_{goj} - N_{thj} ln\left(\frac{N_{goj} - N_{thj}}{N_{goj}} \right) \right] \tag{10}$$

The duration of pulse can be estimated by

$$\tau_j = \frac{E_j}{P_j} \tag{11}$$

4 Results and Discussion

After the verification steps mentioned in the methodology paragraph. Software computer program has been prepared in this study. The rate equations solved numerically by Rung-Kutta -Fehelberg method to simulate the effect of SA ions density on characteristics of the dual generation of passive Q-switched Laser Pulses from laser system consist of $N^{+3} : YAG$ used as AM and $Cr^{+4} : YAG$ as a SA. The input data has been used in computation reported in Table 1.

Table 1. Input data of computation

Parame.	Value	Parame.	Value
σ_{a1}	$2.8 \times 10^{-19} cm^2$ [18]	σ_{sg1}	$7 \times 10^{-18} cm^2$ [7]
σ_{a2}	$5.1 \times 10^{-20} cm^2$ [19]	σ_{sg2}	$4 \times 10^{-18} cm^2$ [19]
λ_1	$1.064 \mu m$ [12]	σ_{se1}	$2 \times 10^{-18} cm^2$ [20]
λ_2	$0.946 \mu m$ [8]	σ_{se2}	$1.1 \times 10^{-18} cm^2$ [19]
γ_1	1 [10]	R_1	0.94
γ_2	2 [10]	R_2	0.99

Figure 3 Show the simulation of the time behavior of the dual passive Q-switching laser pulses which are releases instantaneously from one active medium of passive Q-switching represent 4-levels scheme. One of these pulses related to the spectral transition represent 4-levels scheme which emits 1.064 micrometer wavelength. While the other related to the spectral transition represent 3-levels system which emits 0.964 micrometer laser. It is observed that both pulses are released in

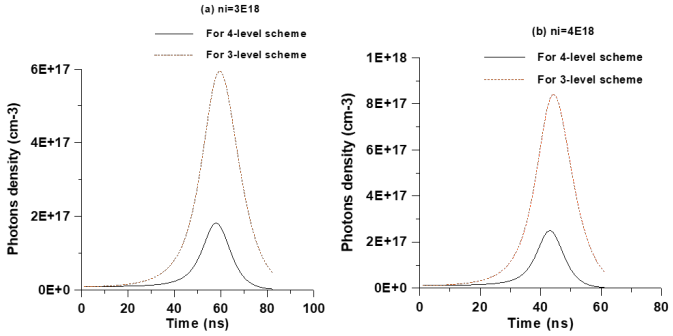

Fig 3. Profile of PQS pulses, which are release from 4 and 3 levels schemes instantaneously as a function of SA ions density

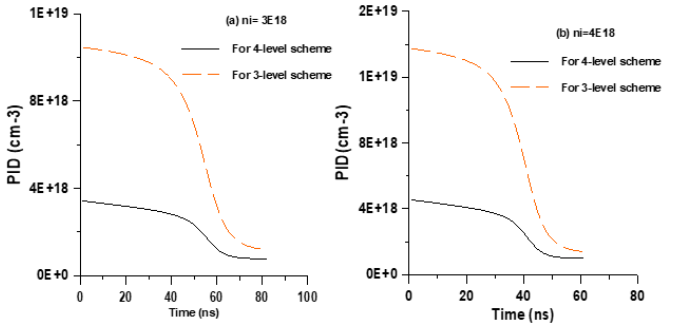

Fig 4. Behavior of population inversion density related from 4 and 3 levels schemes as a function of SA ions density

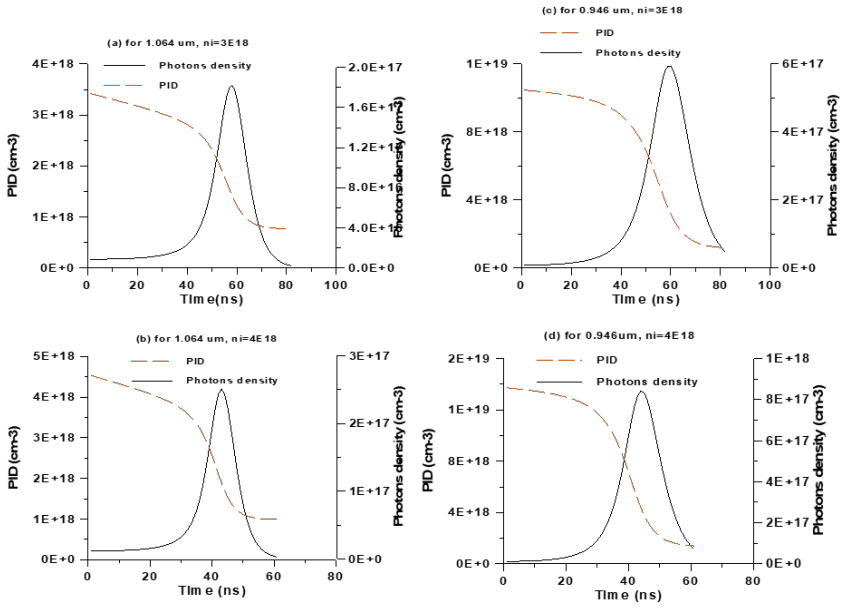

Fig 5. Profiles of PQS pulses, PID as a function of SA ions density (a,b for 4-energy levels, c,d for 3-energy level of AM)

an advanced time as the value of n_i increases as shown in the Figure 3**(a, b)**. The study explains this because of the increase in the values of initial population inversion density of the systems as shown in the Figure 4**(a, b)** and the Figure 5**(a, b, c, d)**.

Figure 6 shows an increase in the initial value of the population inversion density (IPID) of the two levels schemes as a function of SA ions density (cm-3)(n_i), and this behaviour is an enhancement of the study's interpretation of the Figures 3, 4 and 5. Figure 7 represents the difference between the initial and final values of the population inversion density, as we observe an increase in the difference value with an increase of n_i which leads to increase the density number of pulses photons.

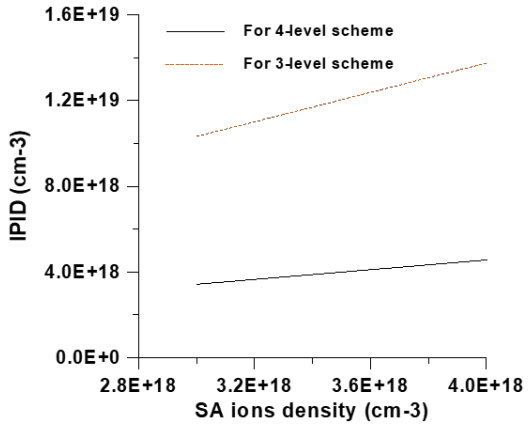

Fig 6. IPID as a function of SA ions density

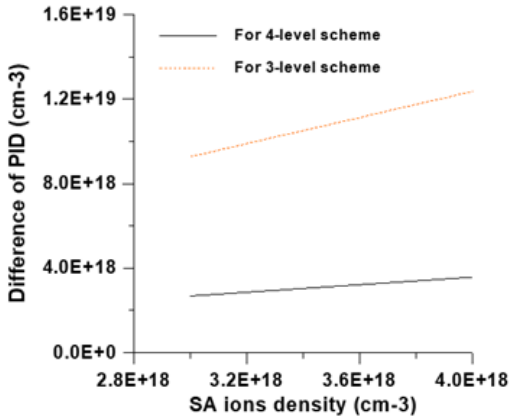

Fig 7. Difference of PID as a function of SA ions density

The characteristics (duration, energy, and the power) of both PQS pulses have been simulated. Figure 8 shows decreasing in duration of both pulses as a function of SA ions density. The study explains this because of the rapid construction of both pulses. This is demonstrated by decreasing the rising time as shown in Figure 9, and the decreasing in the falling time as shown in Figure 10. Figure 11 shows the increasing in the energy of both pulses by increasing n_i. The study explains this because of the increased the initial value of the population inversion density as shown in Figure 6, which resulted in an increase in the maximum value of each pulse's photons as shown in Figure 12. Figure 13 shows the increased value of each pulse's power by increasing n_i. The study explains this because of increased energy and decreased duration time of both pulses as shown in Figures 11 and 8.

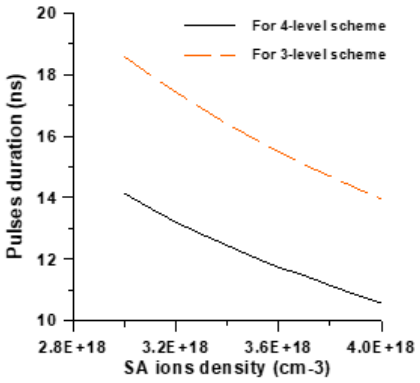

Fig 8. Pulse duration as a function of SA ions density (cm^{-3})

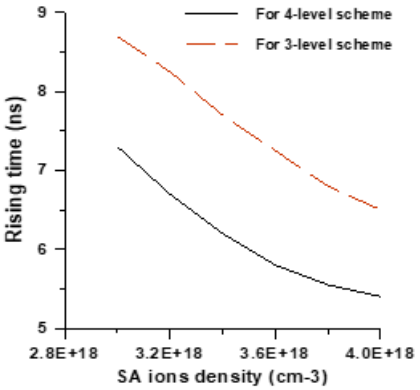

Fig 9. Rising time as function of SA ions density (cm^{-3})

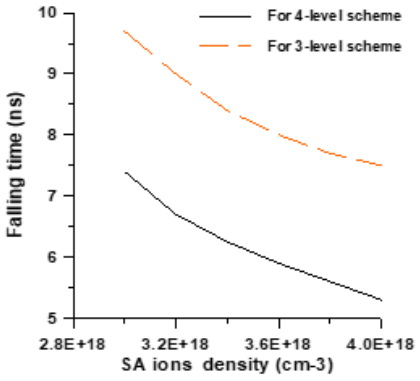

Fig 10. Falling time as a function of SA ions density (cm^{-3})

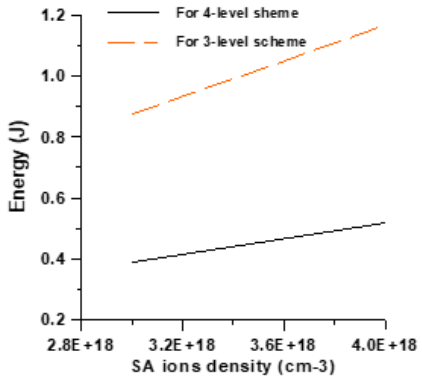

Fig 11. Pulse energy as a function of SA ions density (cm^{-3})

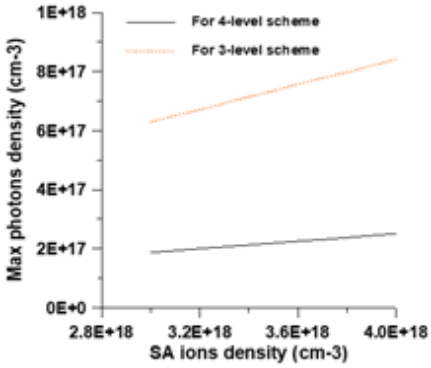

Fig 12. Max.of Photons density as a function of SA ions density (cm^{-3})

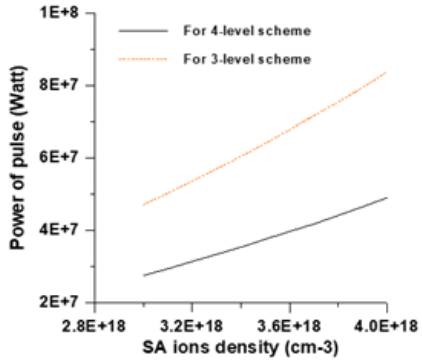

Fig 13. Pulse power as a function of SA ions density (cm^{-3})

5 Conclusions

1- The mathematical model presented in this study suitable in related studies on the generation of passive Q-switching laser pulses. Physically and mathematically, it is established to employ the spectral lines of gain medium that form four level energy or quasi three level energy laser systems.2- The increasing of ions density of SA leads to increase the energy of the dual passive q-switching laser pulses, while the duration decrease as a function of ions density of SA, which provides a good chance of getting high power laser pulses. Where was the energy, duration, and the power of PQS pulse at $1.064um$ are $0.388J, 14.134ns 2.745 \times 10^7$ Watt respectively at $ni = 3 \times 10^{18} cm^{-3}$, while for $ni = 4 \times 10^{18}$ the energy, duration, and the power have become $0.518J, 10.572ns, 4.898 \times 10^7 Watt$ respectively. It has been noted for $0.964um$, that the energy, duration, and the power of PQS pulse are $0.875J, 18.58ns, 4.709 \times 10^7$ Watt respectively at $ni = 3 \times 10^{18} cm^{-}$ 3, while for $ni = 4 \times 10^{18}$ the energy, duration, and the power have become $1.169J, 13.94ns$, 8.38×10^7 Watt respectively.

References

1) Pérez-Alonso V, Weigand R, Sánchez-Balmaseda M, Pérez JMG. Powerful algebraic model to design Q-switched lasers using saturable absorbers. *Optics & Laser Technology*. 2023;164:1–13. Available from: https://doi.org/10.1016/j.optlastec.2023.109506.
2) Zhang X, Zhong K, Qiao H, Li F, Zheng Y, Xu D, et al. Passively Q-Switched Dual-Wavelength Laser Operation With Coaxially End-Pumped Composite Laser Materials. *IEEE Photonics Journal*. 2021;13(6):1–7. Available from: https://doi.org/10.1109/JPHOT.2021.3120000.
3) Wang J, Xie L, Wang Y, Lan Y, Wu P, Lv J, et al. High-damage vanadium pentoxide film saturable absorber for sub-nanosecond Nd:YAG lasers. *Infrared Physics & Technology*. 2023;129:104580. Available from: https://doi.org/10.1016/j.infrared.2023.104580.
4) Zeng KK, Wu X, Jiang F, Zhang J, Kong J, Shen J, et al. Experimental research on micro hole drilling of polycrystalline Nd:YAG. *Ceramics International*. 2022;48(7):9658–9666. Available from: https://doi.org/10.1016/j.ceramint.2021.12.165.
5) Zhao ZY, Cai ZT, Zhao CM, Zhang J. Solar-pumped 1061-/1064-nm dual-wavelength Nd:YAG monolithic laser. *Journal of Photonics for Energy*. 2023;62(3). Available from: https://doi.org/10.1117/1.OE.62.3.036103.
6) Payziyev S, Sherniyozov A. Influence of thermal population of lower laser levels on the performance of end-side-pumped Ce:Nd:YAG solar laser. *Journal of Photonics for Energy*. 2022;12(04):44501. Available from: https://doi.org/10.1117/1.JPE.12.044501.
7) Giese A, Körber M, Kostourou K, Kopf D, Kottcke M, Lohbreier J, et al. Passively Q-switched sub-100 ps Yb3+:YAG/Cr4+:YAG microchip laser: experimental results and numerical analysis. *Solid State Lasers XXXII: Technology and Devices*. 2023;12399:187–197. Available from: https://doi.org/10.1117/12.2649057.
8) Tang J, Bai Z, Zhang D, Qi Y, Ding J, Wang Y, et al. Advances in All-Solid-State Passively Q-Switched Lasers Based on Cr4+:YAG Saturable Absorber. *Photonics*. 2021;8(4):1–14. Available from: https://doi.org/10.3390/photonics8040093.
9) Tanaka H, Kränkel C, Kannari F. Transition-Metal-Doped Saturable Absorbers For Passive Q-Switching Of Visible Lasers. *Optical Materials Express*. 2020;10(8):1827–1842. Available from: https://doi.org/10.1364/OME.395893.
10) Wang P, Zhu C. Passively Q-Switched and Mode-Locked Fiber Laser Based on a Zeolitic Imidazolate Framework-67 Saturable Absorber. *Frontiers in Physics*. 2022;10:1–8. Available from: https://doi.org/10.3389/fphy.2022.926344.
11) Hassan AA, Wahid SNA, Hamood HY. Numerical modeling of passively Q-switched Nd: YAG lasers with Cr+4: YAG as a saturable absorber. *Journal of Xidian University*. 2021;15(2):36–42. Available from: https://doi.org/10.37896/jxu15.2/005.
12) Li M, Qin Y, Wang C, Liu X, Long S, Tang X, et al. Nonuniform pumped passively Q-switched laser using Nd:YAG/Cr4+:YAG composite crystal with high-pulse energy. *Optical Engineering*. 2019;58(03). Available from: https://doi.org/10.1117/1.OE.58.3.036106.
13) Hussein TM, Salih AKM. Simulation of Effective Beam Area Ratio Effect on Characteristics of Passive Q-Switched Fiber Doped Laser. *Journal of Optoelectronics Laser*. 2022;41(10):452–461. Available from: http://www.gdzjg.org/index.php/JOL/article/view/1286.
14) Hussein ZA, Salih AKM. Saturable absorber initial transmission effect on characteristics of passive Q-switching Er+3 doped fiber laser. In: 3RD INTERNATIONAL SCIENTIFIC CONFERENCE OF ALKAFEEL UNIVERSITY (ISCKU 2021), 22–23 March 2021, Najaf, Iraq;vol. 2386, Issue 1 of AIP Conference Proceedings. 2022. Available from: https://doi.org/10.1063/5.0067126.
15) Zhang X, Zhong K, Qiao H, Zheng Y, Li F, Xu D, et al. A passively Q-switched dual-wavelength laser with pulsed LD coaxial end-pumped configuration. *Advanced Lasers, High-Power Lasers, and Applications XIII*. 2022;12310. Available from: https://doi.org/10.1117/12.2641747.
16) Tarkashvand M, Farahbod AH, Hashemizadeh SA. Study of the Spatiotemporal Behavior of LED-Pumped Ce:Nd:YAG Laser. *International Journal of Optics and Photonics*. 2020;14(1):75–84. Available from: https://ijop.ir/article-1-396-en.pdf.
17) Nady A, Aly E. Studies on Q- switching and Mode- Locking Pulse Generation Fiber Cavity with Saturable Absorber. 2017. Available from: https://www.semanticscholar.org/paper/Studies-on-Q-switching-and-mode-locking-pulse-in-Nady-Aly/ea4ed9307ae4f0d52885763b42442016489c3c7c.
18) Zhang B, Chen Y, Wang P, Wang Y, Liu J, Hu S, et al. Direct bleaching of a Cr4+:YAG saturable absorber in a passively Q-switched Nd:YAG laser. *Applied Optics*. 2018;57(16):4595–4600. Available from: https://doi.org/10.1364/AO.57.004595.
19) Gürel Ö. Development of a UV Source Based on Frequency Quadrupling of a Q-switched Nd:YAG Laser. Stockholm, Sweden. 2009. Available from: https://www.aphys.kth.se/polopoly_fs/1.422571.1600689849!/Menu/general/column-content/attachment/G%C3%BCrel_msc_thesis_2009.pdf.
20) Koechner W. Solid-State Laser Engineering. Springer. 2013. Available from: https://www.hazemsakeek.net/wp-content/uploads/2021/06/Optical-Amplification-arabic.